Joint ERCOFTAC/EU-CTFF
European Drag Reduction and Flow Control Meeting – EDRFCM 2022
September 6$^{\text{th}}$–9$^{\text{th}}$, 2022, Paris, France

DRAG REDUCTION ON A TRANSONIC WING

Maurizio Quadrio
Dip. Scienze e Tecnologie Aerospaziali, Politecnico di Milano, 20156 Milano, Italy

Alessandro Chiarini
Dip. Scienze e Tecnologie Aerospaziali, Politecnico di Milano, 20156 Milano, Italy

Davide Gatti
Institute for Fluid Mechanics, Karlsruhe Institute of Technology, 76131 Karlsruhe, Germany

Jacopo Banchetti
Dip. Scienze e Tecnologie Aerospaziali, Politecnico di Milano, 20156 Milano, Italy

Antonio Memmolo
High Performance Computing Department, CINECA, 40033 Bologna, Italy

Sergio Pirozzoli
Dipartimento di Ingegneria Meccanica e Aerospaziale, Roma La Sapienza Univ, 00184 Roma, Italy

ABSTRACT

Skin-friction drag reduction is applied to a transonic wing to modify its aerodynamic performance. A Direct Numerical Simulations with up to 1.8 billions cells of the compressible flow around a wing slab is presented, at $Re_\infty = 3 \times 10^5$ and $M_\infty = 0.7$. Control is applied only on a limited portion of the suction side of the wing via streamwise-travelling waves of spanwise forcing. Besides locally reducing friction, control modifies the shock wave, significantly increasing the global efficiency of the wing. The increased efficiency implies that the airplane can fly at a lower angle of attack and, therefore, with a lower drag. Estrapolating the benefits at the airplane level yields 9% reduction for the drag coefficient of the aircraft, with negligible energy cost from the active control.

BACKGROUND

Most of the research on skin-friction drag reduction has taken place in plane wall flows, where drag is entirely made by viscous friction. In more complex flows, where additional contributions to drag are present (pressure drag, parasitic drag, separation, lift-induced drag and wave drag), reducing the total drag is the goal. At EDRFCM 2017 we proposed [4] that localized friction reduction (specifically obtained via spanwise forcing) might bring in substantial advantages in aeronautical configurations; and at EDRFCM 2019 [3] we described how skin-friction drag reduction enables additional pressure drag reduction for a non-planar wall flow in the incompressible regime [2]. The idea is now being explored [1].

In this work we present the first direct numerical simulation (DNS) of the compressible turbulent flow over a wing slab in the transonic regime with flow control. We explore to what extent a localised control for skin-friction reduction alters the aerodynamic performances of the wing; the results will be extrapolated to the entire airplane. The active control technique chosen for the study is the streamwise-traveling waves of spanwise forcing [6], which offers the double advantage of producing large (hence easily measurable) effects and large net savings. However, the general conclusions are valid for any skin-friction reduction technology.

METHODS

We consider by DNS the transonic flow around a wing slab made by a supercritical airfoil. The Reynolds and Mach numbers of the flow are $Re_\infty = U_\infty c/\nu_\infty = 3 \times 10^5$ and $M_\infty = U_\infty/a_\infty = 0.7$, where c is the airfoil chord and U_∞, ν_∞ and a_∞ are the free-stream velocity, kinematic viscosity and sound speed. The angle of attack is $\alpha = 4^\circ$, which corresponds to the maximum aerodynamic efficiency of the profile. The DNS code [5] solves the compressible Navier–Stokes equations for a calorically perfect gas. The incoming flow is laminar, and transition to turbulence is enforced on both sides of the airfoil via a volume force located at $x = 0.1c$.

On a portion of the suction side of the wing, streamwise-travelling waves of spanwise velocity are applied. The spanwise velocity component w_w at the wall is:

$$w_w(x,t) = f(x) A \sin(\kappa_x x - \omega t)$$

where A is the maximum forcing amplitude and κ_x, ω are the spatial and temporal frequencies of the wave. A smoothing function $f(x)$ is used to raise the spanwise velocity at the initial position x_s and then return it to zero at x_e. Two control cases, C1 and C2, are considered. Both are of moderate intensity, with forcing applied locally on the mid portion of the suction side; however, slight changes in A, x_s, x_e render control C2 more effective (higher intensity and wider extension).

DNS are carried out with/without control on two meshes: the baseline grid has 536 million cells, and a finer grid with 1.8 billions cells is used for validation. The finest grid has $N_x, N_y, N_z = 6144, 768, 384$ cells.

RESULTS

An overview of the instantaneous fields is given in figure 1, where vortical structures for the no-control case are visualised via isosurfaces of the imaginary part of the complex conjugate eigenvalue pair of the velocity gradient tensor $\Im(\lambda_{ci})$. The three sonic lines at $M = 1$ are shown for the no-control (red), C1 (blue) and C2 (green) cases. The flow becomes supersonic at the nose and remains laminar up to the tripping. The supersonic region extends up to $x \approx 0.5c$, where the flow undergoes abrupt recompression due to the shock wave. The control moves the shock wave downstream and enlarges the supersonic region, and increases the shock wave intensity. Consistently, the maximum Mach number increases from $M = 1.087$ (no-control) to $M = 1.093$ (C1) and $M = 1.116$ (C2), while its position remain almost unchanged. All these changes are consistent with a decreased friction in the actuated region.

Figure 2 plots the mean friction and pressure coefficients. Since on the pressure side there is no actuation, the curves are virtually unchanged. In the controlled cases, after x_s the forcing effectively reduces friction in the actuated region. A short spatial transient is required [7] for drag reduction to develop. In both cases, c_f becomes negative after the shock wave. Unlike c_f, control modifies c_p even outside the actuated region. Two distinct control effects are observed: (i) the compression associated with the shock wave is moved downstream and (ii) the expansion at the leading edge is stronger, leading to a plateau with lower c_p. The recirculating region in the controlled cases decreases the adverse pressure gradient in the area close to the shock; see the milder slope of c_p in correspondence of the pressure recovery before the shock-induced compression. Thus the shock wave moves downstream and enlarges the supersonic bubble, resulting in an increase of the velocity within the bubble and, therefore, into more intense expansion in the fore part of the airfoil. Both effects are more evident in C2, that is stronger and designed to produce an evident recirculation after the shock wave. Overall, the control effect on c_p can be assimilated to that of an increase of the free-stream Mach number, but only for the suction side.

The control-induced changes in the distributions of friction and pressure positively affect both lift and drag. The combined changes of friction and pressure result into a reduction of the total drag for both cases, quantified by 4.5% for C1 and by a marginal 0.8% for C2. However, the crucial control effect is the increase of the lift coefficient, by 1.5% for C1 and 11.3% for C2. The wing efficiency, therefore, is significantly enhanced in both cases, by 6.8% for C1 and 13.5% for C2. Increased wing efficiency implies that the required lift can be obtained at a lower angle of attack α and, therefore, at the cost of a lower drag. By running a further DNS at the smaller angle of attack required to achieve the same lift, a total drag reduction of almost 15% is obtained.

At the Meeting we will show how these figures can be scaled up to the airplane level: the outcome is that the energy cost of the active control, once deployed only on a fraction of the surface, becomes negligible. Its effects, though, remain finite, and we estimate a 9% for the entire airplane in cruise flight.

Although demonstrated for spanwise forcing only, the idea behind the present results is general and valid for any type of control, including passive strategies, e.g. riblets. Moreover, the study is just a first attempt and should not be taken as indicative of the maximum achievable gain: design and placement of skin-friction control devices over a complex body for drag reduction is a new optimization problem that might yield interesting outcomes. Considering skin-friction drag reduction as a tool and not only as a goal in flows where friction drag is not the key target for optimisation will open new avenues to a widespread use of flow control.

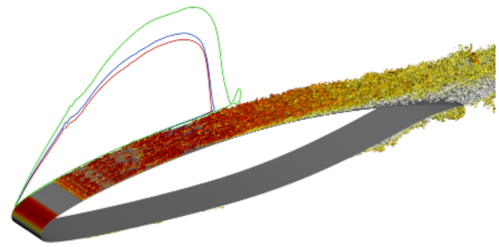

Figure 1: Isosurfaces of the swirling strength $\Im(\lambda_{ci}) = 100$ in the no-control case, coloured with the kinetic energy k with a white-to-red colormap in the range $0 \leq k \leq 1$. Lines are the sonic line $M = 1$ for reference (red), C1 (blue) and C2 (green)

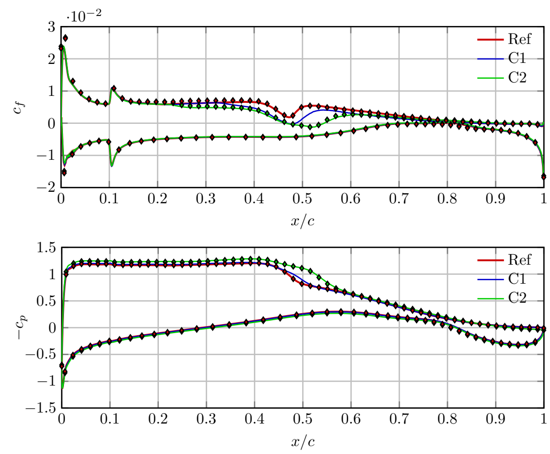

Figure 2: Friction coefficient c_f (top) and pressure coefficient c_p (bottom). Reference and C2 results obtained on the finer grid are shown with symbols. Tripping is at $x/c = 0.1$. Forcing starts at $x/c = 0.3$ for C1 and $x/c = 0.2$ for C2, and ends at $x/c = 0.78$ for both.

REFERENCES

[1] M. Albers and W. Schröder. Lower drag and higher lift for turbulent airfoil flow by moving surfaces. *International Journal of Heat and Fluid Flow*, 88:108770, April 2021.

[2] J. Banchetti, P. Luchini, and M. Quadrio. Turbulent drag reduction over curved walls. *J. Fluid Mech.*, 896:1–23, August 2020.

[3] J. Banchetti and M. Quadrio. Turbulent drag reduction for a wall with a bump. In *17th EDRFCM, Bad Reichenhall*, 2019.

[4] A. Gadda, J. Banchetti, G. Romanelli, and M. Quadrio. Drag reduction of a whole-aircraft configuration via spanwise forcing. In *16th EDRFCM, Monteporziocatone*, 2017.

[5] A. Memmolo, M. Bernardini, and S. Pirozzoli. Scrutiny of buffet mechanisms in transonic flow. *Int. J. Numer. Methods Heat Fluid Flow*, 28(5):1031–1046, January 2018.

[6] M. Quadrio, P. Ricco, and C. Viotti. Streamwise-traveling waves of spanwise wall velocity for turbulent drag reduction. *J. Fluid Mech.*, 627:161–178, 2009.

[7] M. Skote. Temporal and spatial transients in turbulent boundary layer flow over an oscillating wall. *Int. J. Heat Fluid Flow*, 38:1–12, 2012.